Gold anode corrosion in aqueous solution of 1,2-diaminopropane with formation of colloidal gold nanoparticles

M. D. Vedenyapina, V. V. Kuznetsov, N. N. Makhova, and D. I. Rodikova*

N. D. Zelinsky Institute of Organic Chemistry, Russian Academy of Sciences,
47 Leninsky prosp., 119991 Moscow, Russian Federation.
E-mail: mvedenyapina@yandex.ru

The kinetics and mechanism of corrosion of Au anode in a weakly basic aqueous solution of 1,2-diaminopropane were studied by gravimetry. According to transmission electron microscopy data, the products of anode corrosion under galvanostatic conditions are reduced on the steel cathode to give not only the electrolytic Au deposit on the cathode, but also colloidal gold nanoparticles in the electrolyte medium. A mixture of four gold complexes with 1,2-diaminopropane was isolated from the reaction solution; the ratio of the complexes and the structure of the predominant complex were proposed on the basis of NMR spectra.

Key words: 1,2-diaminopropane, gold, electrodes, kinetics, corrosion, nanoparticles, colloidal gold, complex compounds.

The development of methods for the recovery of gold from ores aimed at replacing toxic potassium cyanide includes the search for safer reagents, which has been carried out for several years. Among these reagents, the best studied are thiourea and thiosulfate,[1—6] which provide the recovery of gold *via* the formation of gold complexes. Mercaptoacetic and *meso*-2,3-dimercaptosuccinic acid were also tested as ligands for the formation of gold complex compounds.[7] Previously,[8—13] we described and studied the anodic corrosion of a gold electrode in weakly basic aqueous solutions (0.05 *M* K_2CO_3) of several organic bases: hexahydropyrimidine (**1**),[8] 1,5-diazabicyclo[3.1.0]-hexane (**2**),[8,9] 6-methyl-1,5-diazabicyclo[3.1.0]hexane (**3**),[8,9] 6,6-dimethyl-1,5-diazabicyclo[3.1.0]hexane (**4**),[8,9] 1,3-diaminopropane (**5**),[10,11] ethylenediamine (**6**),[11,12] and 1,4-diaminobutane (**7**).[11,13]

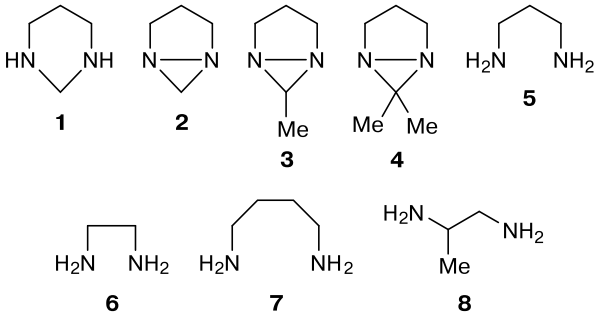

In these studies, the phenomenon of corrosion of Au electrode in solutions of diamines **1**—**7** and gold transfer to the cathode giving a compact deposit were investigated using gravimetric analysis. The results of measurements (the difference between the anode and cathode masses) can be used to calculate the mass of gold that is present in the solution at any time point of electrolysis. In some cases, the products formed during corrosion, which represented gold complexes with the corresponding ligands, were isolated.

For detailed investigation of the mechanism of gold corrosion in solutions of diamines, we chose the following diaminoalkanes:[11] 1,3-diaminopropane (1,3-DAP, **5**), ethylenediamine (EDA, **6**), 1,4-diaminobutane (1,4-DAB, **7**), and 1,2-diaminopropane (1,2-DAP, **8**). The electrochemical behavior of the amines in a weakly basic aqueous solution was studied by cyclic voltammetry (CV). Comparative analysis of the behavior of the Au anode in solutions of these compounds demonstrated that 1,2-diaminoalkanes **6** and **8** are strongly adsorbed on the gold anode and completely block the anode surface, whereas 1,3- and 1,4-diaminoalkanes **5** and **7** are not prone to such strong adsorption. Therefore, a linear dependence of the anode peak currents on the potential scan rate was observed only for these 1,2-diaminoalkanes.

The corrosion of Au anode in aqueous solutions was studied by gravimetric measurements only for diamines **5**—**7**, while for 1,2-diaminopropane **8** this study was not carried out. Although the 1,2-DAP molecule, like EDA **6** molecule, contains amino groups connected by an ethylene bridge, 1,2-DAP may be expected to coordinate gold more efficiently than EDA because of the $+I$ effect of the methyl substituent in the aliphatic part of the molecule.

This communication describes a gravimetric study of the kinetics and mechanism of corrosion of a gold anode in an aqueous solution of 1,2-diaminopropane **8**.

Published in Russian in *Izvestiya Akademii Nauk. Seriya Khimicheskaya,* No. 10, pp. 1884—1891, October, 2020.

Experimental

Commercial 1,2-diaminopropane **8** (ACROS) was used. The working solutions were prepared using doubly distilled water. Pure for analysis grade K_2CO_3 was used.

The anodic corrosion of gold was conducted in an undivided two-electrode cell. Gold and steel wires 0.3 mm in diameter immersed into an electrolyte solution by 15 mm served as the anode and cathode, respectively. Electrolysis was carried out in the galvanostatic mode. The concentration of 1,2-DAP in a 0.05 *M* solution of K_2CO_3 was 1.0 mol L^{-1}; the volume of the working solution was 20 mL. The electrodes were weighed on an ABJ220-4NM electronic analytical balance (Kern, USA) (d = 0.0001 g).

For isolation of the product formed during electrolysis (Au anode corrosion in a 1,2-DAP solution), the reaction solution was left in an open glass crystallization dish at room temperature for 2—3 days until water completely evaporated. The resulting solid residue containing a mixture of coordination compounds **9a—d** was extracted with methanol (2×50 mL), then the solvent was evaporated, and the solution was kept in an open glass crystallization dish for ~24 h at ~30 °C.

The IR spectra of the initial 1,2-DAP were measured in thin layer between KBr plates, and the IR spectra of the obtained mixture of coordination compounds **9a—d** were recorded for a sample obtained by pressing compounds with KBr on a Bruker Alpha instrument.

The ^{1}H NMR spectra of the initial 1,2-DAP and a mixture of gold complexes with 1,2-diaminopropane **9a—d** were recorded on a Bruker AM-300 spectrometer (operating at 300 MHz) and the ^{13}C NMR spectra were run on a Bruker AM-300 spectrometer (operating at 75.47 MHz). The signal positions in the ^{1}H NMR spectra were referred to the residual protons of the deuterated solvent (D_2O).

1,2-Diaminopropane (1,2-DAP, 8). IR (KBr), ν/cm^{-1}: 424, 476, 511, 617, 668, 753, 814, 915, 954, 1066, 1109, 1239, 1280, 1305, 1383, 1457, 1597, 1733, 2341, 2360, 2870, 2928, 2960, 3191, 3282, 3355. ^{1}H NMR (D_2O, δ, J/Hz, ν/Hz): 1.21 (d, 3 H, Me, ^3J = 6.5 Hz); 2.60—2.67 (dd, 1 H, NC$\underline{H}_A$—, ABX system, Δν = 31.5 Hz, ^2J = 12.8 Hz, ^3J = 6.9 Hz); 2.69—2.75 (dd, 1 H, NC$\underline{H}_B$—, ^2J = 12.8 Hz, ^3J = 5.5 Hz); 2.96—3.06 [m, 1 H, NC$\underline{H}$(Me)—].

Gold complexes with 1,2-DAP 9a—d. IR spectrum of the mixture of complexes, ν/cm^{-1}: 437, 466, 644, 700, 818, 886, 933, 974, 1039, 1059, 1118, 1169, 1197, 1232, 1278, 1324, 1379, 1401, 1439, 1478, 1578, 1655, 2215, 2345, 2567, 2671, 2871, 2931, 2962, 3310.

Complex [Au^{n+}(H$_2$NCH(Me)CH$_2$NH$_2$)$_4$](CO$_3^{2-}$)$_{0.5n}$ (9a), (65%). ^{1}H NMR (D_2O, δ, J/Hz, ν/cm^{-1}): 1.12 (d, 12 H, Me, ^3J = 6.7 Hz); 2.95—3.16 (dd, 4 H, NC$\underline{H}_A$—, ABX system, Δν = 40.4 Hz, ^2J = 14.8 Hz, ^3J = 7.7 Hz); 3.09—3.16 (dd, 4 H, NC$\underline{H}_B$—, ^2J = 14.8 Hz, ^3J = 4.2 Hz); 3.21—3.31 (m, 4 H, NC$\underline{H}$(Me)—).

Complex [Au^{n+}(H$_2$NCH(Me)CH$_2$NH$_2$)$_3$](CO$_3^{2-}$)$_{0.5n}$ (9b), (15%). ^{1}H NMR (D_2O, δ): 1.09 (d, 9 H, Me, ^3J = 7.0 Hz); 2.95—3.16 (dd, 3 H, NC$\underline{H}_A$—); 3.09—3.16 (dd, 3 H, NC$\underline{H}_B$—); 3.21—3.31 (m, 3 H, NC$\underline{H}$(Me)—).

Complex [Au^{n+}(H$_2$NCH(Me)CH$_2$NH$_2$)$_2$](CO$_3^{2-}$)$_{0.5n}$ (9c), (15%). ^{1}H NMR (D_2O, δ): 1.02 (d, 6 H, Me, ^3J = 6.8 Hz); 2.65—2.80 (dd, 4 H, NCH_2—); 3.21—3.31 (m, 2 H, NC$\underline{H}$(Me)—).

Complex [Au^{n+}(H$_2$NCH(Me)CH$_2$NH$_2$)](CO$_3^{2-}$)$_{0.5n}$ (9d), (5%). ^{1}H NMR (D_2O, δ): 0.92 (d, 3 H, Me, ^3J = 6.5 Hz); 2.82—2.95 (dd, 2 H, NCH_2—); 3.21—3.31 (m, 1 H, NC$\underline{H}$(Me)—).

Table 1. Chemical shifts of carbon atoms in the ^{13}C NMR spectrum (D_2O) of 1.2-diaminopropane **8** and ligands in complexes **9a—d**

Compound	Carbon chemical shifts δ		
	Me	—CH—	—CH$_2$—
8	21.2	49.4	50.1
9a (65%)	16.8	49.4	46.0
9b (15%)	18.5	49.4	46.2
9c (15%)	19.2	48.2	46.7
9d (5%)	19.4	48.6	47.9

The positions of carbon signals in the ^{13}C NMR spectrum of the starting free 1,2-DAP and ligands in the formed complexes **9a—d** are summarized in Table 1.

The microstructure of electrodes and solid products isolated after the electrolysis of gold in an aqueous solution of 1,2-DAP was examined by field emission scanning electron microscopy (FE-STEM) on a Hitachi SU8000 electron microscope (Japan). The images were obtained in the secondary electron mode at an accelerating voltage of 2—30 kV and a working distance of 8.4—11.0 mm. The energy dispersive X-ray spectroscopy investigation of samples was performed using an Oxford Instruments X-max energy dispersion spectrometer (UK). The samples of solid products isolated after the electrolysis of 1,2-DAP were fixed by conductive adhesive tape and the electrode samples were placed on an aluminum table 25 mm in diameter and fastened by two screws.

Elemental analysis was carried out on a PerkinElmer 2400 CHN analyzer (USA). The colloidal gold particles formed after electrolysis of the gold anode in an aqueous solution of 1,2-diaminopropane **8** were examined by transmission electron microscopy (TEM) using an Hitachi HT7700 electron microscope (Japan). The images were recorded in the transmission (bright field) mode at an accelerating voltage of 100 kV. Prior to the measurement, the working solution was deposited on a thin carbon film attached to a copper grid 3 mm in diameter. The grid was mounted in a special holder. The sample was deposited as a liquid and then dried *in vacuo*. The analytical measurements were optimized using the approach described earlier.[14]

Results and Discussion

The electrolysis conducted in a 1,2-DAP solution at a 10 mA current on a gold electrode demonstrated that the anode undergoes corrosion with mass loss, as was noted previously.[8—10,12,13] As this takes place, metallic gold is deposited on the cathode (steel wire). The kinetics of mass loss of the gold anode (m_{corr}) and mass gain of the cathode deposit (m_{dep}) are illustrated in Fig. 1. The mass of gold present in the working solution (m_{sol}) was calculated as the difference of these values. It was shown that during electrolysis, the m_{corr} value increases linearly. The mass gain of the cathode deposit is slow in the first 25 h and then linearly increases. The m_{sol} value rapidly increases the first 20 h and then remains almost invariable. A com-

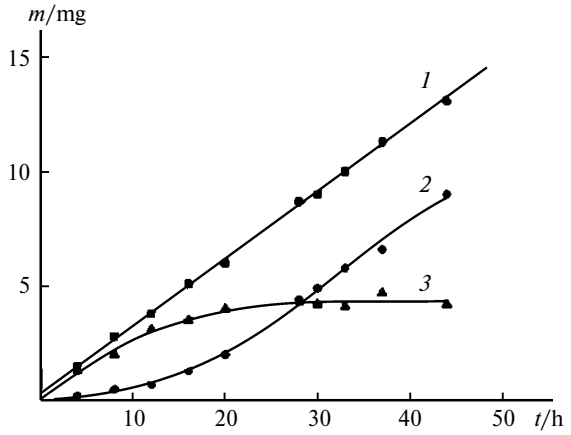

Fig. 1. Kinetics of anodic dissolution of metallic gold in an aqueous solution of 1,2-diaminopropane at 10 mA current and $C = 1.0$ mol L^{-1}; (*1*) weight loss of gold anode (m_{corr}), (*2*) weight of the cathodic deposit of metallic gold (m_{dep}), and (*3*) calculated weight of gold located in an aqueous solution of 1,2-diaminopropane **8** (m_{sol}).

parative analysis of the obtained results and published data[10,12] showed that the situation is similar when other diaminoalkanes are used as ligands. However, it is noteworthy that after the same time of electrolysis, the decrease in the gold anode mass in 1,2-DAP solution was less pronounced than in solutions of 1,3-DAP or EDA, but more pronounced than in a 1,4-diaminobutane solution.

As in previous publications,[8—10,12,13] for interpreting the observed kinetics, the sum of anodic dissolution and cathodic deposition of gold can be represented as a system of differential equations:

$$dm_1/dt = k_1 \quad (1)$$

$$dm_2/dt = k_1 - k_2 m_2 \quad (2)$$

$$dm_3/dt = k_2 m_2 \quad (3)$$

where m_1, m_2, and m_3 are, respectively, the masses of gold migrating from the anode to the solution, deposited from the solution on the cathode, and present in solution at time point t.

Solution of this system of equations using the Mathcad software gave the k_1 and k_2 values that describe most accurately the experimental data (see Fig. 1). The k_1 and k_2 values for 1,2-diaminopropane **8** are 0.31 mg h^{-1} and 0.06 h^{-1} (Table 2).

Comparison of these results with the results of calculations of the constants for 1,3-DAP and ethylenediamine[10,12] indicates that corrosion in an aqueous solution of 1,2-DAP proceeds more slowly and with more difficulty. According to the value of k_2, the intensity of the electrochemical process on the cathode with participation of this ligand is intermediate between those of ethylenediamine **6** and 1,3-diaminopropane **5** (see Table 2).

Electron microscopic examination showed the corrosion of gold anode taking place during electrolysis in a 1,2-DAP solution (Fig. 2, *a*) and the cathodic deposit of dendritic gold formed on the steel cathode surface (Fig. 2, *b*). An energy dispersive X-ray spectroscopy study of the chemical composition of the steel cathode surface showed the presence of Au. Like in the case of EDA or 1,3-DAP, no nitrogen was detected on the anode surface upon corrosion in a 1,2-diaminopropane **8** solution.

After electrolysis of a solution of 1,2-DAP **8** with a gold anode, we analyzed the obtained products of electrolysis in the working solution before and after extraction by the methods described below. When corrosion of the gold anode in a 1,2-DAP solution is carried out at 10 mA current, a gold deposit is formed on the cathode and the solution becomes intensely yellow colored. The solution was studied by transmission electron microscopy (TEM). In the obtained micrograph (Fig. 3), one can see round-shaped colloidal gold particles of 20—70 nm size. After methanol extraction of the products of electrolysis (coordination compounds) from the working solution, colloidal gold particles cannot be detected by TEM. Apparently, in this case, destabilization of the colloidal system takes place.

The ^{1}H NMR spectrum of free 1,2-diaminopropane **8** exhibits one doublet with $\delta = 1.21$ for the Me protons (Fig. 4, *a*). The $\delta = 0.91$—1.13 range of the ^{1}H NMR spectrum of the product of Au anode corrosion in 1,2-DAP shows four doublets for methyl protons with $\delta = 0.92$, 1.02, 1.09, and 1.12 ppm and integrated intensity ratio of

Table 2. Kinetic and electrochemical characteristics of gold corrosion in aqueous solutions of diaminoalkanes

Diamine	k_1/mg h^{-1}	k_2/h^{-1}	E_a/mV	I_a/mA	E_c/mV	I_c/mA	Dissolution rate /mg cm^{-2} h^{-1}
8	0.31	0.06	600	50	91	−51	4.76
5[a]	0.42	0.04	680	26	110	−22	6.66
6[b]	0.55	0.11	572	63	105	−74	8.73

Note. E_a, E_c are current peak potentials in the anodic and cathodic CV branches,[4] I_a, I_c are current peaks in the anodic and cathodic CV branches.[4]

[a] Data of Ref. 3.

[b] Data of Ref. 5.

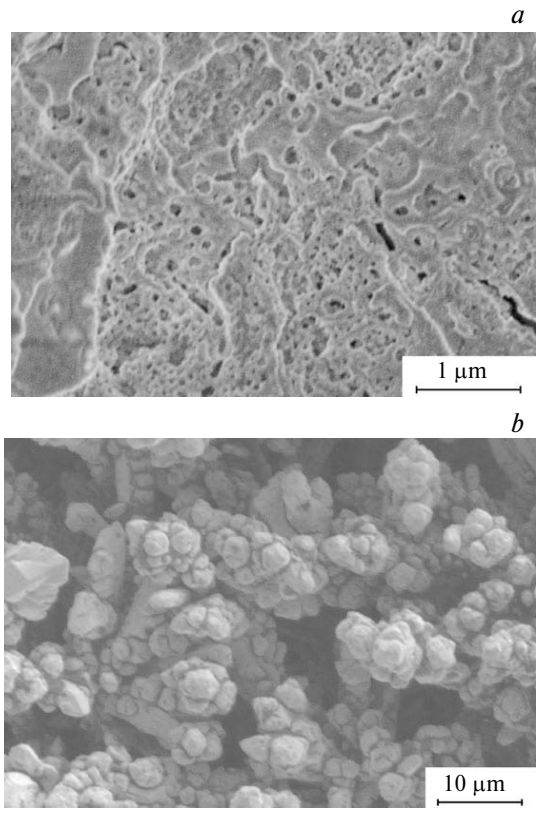

Fig. 2. SEM images of the gold anode surface (*a*) and steel cathode surface with a cathodic gold deposit (*b*) after the electrolysis in an aqueous solution of 1,2-diaminopropane **8**.

5 : 15 : 15 : 65% (Fig. 4, *b*). It is evident that the Me proton signals of the corrosion products are shifted upfield by $\Delta\delta = 0.21$, 0.19, 0.12, and 0.09, respectively. This attests to the formation of four gold complexes of 1,2-DAP (**9a—d**), which probably differ in the number of ligand molecules bound to the Au atom.

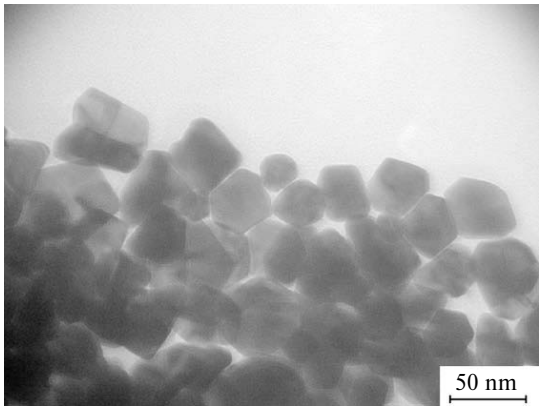

Fig. 3. TEM image of colloidal gold particles obtained after electrolysis of a gold anode in an aqueous solution of 1,2-diaminopropane **8**.

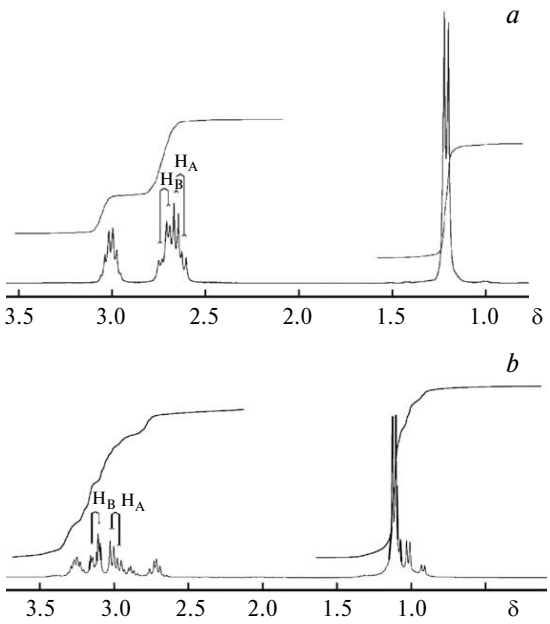

Fig. 4. Fragment of the ^{1}H NMR spectrum of 1,2-diaminopropane **8** in D_2O (*a*) and complexes $[Au^{n+}(H_2NCH(Me)CH_2NH_2)_m](CO_3^{2-})_{0.5n}$ (**9a—d**) in D_2O (*b*).

The ability of gold to form simultaneously several coordination compounds with different numbers of the same ligand was demonstrated previously.[15] The upfield (rather than downfield) shift of the signals for the ligand methyl protons is probably attributable to the back-donation of the π-electrons of gold d-orbital to the ligand. It is known[16—18] that back donation of π-electrons increases shielding of the ligand atoms in the complex and induces upfield shifts of the ligand proton signals in the ^{1}H NMR spectrum. It is evident that the highest back donation will be observed when the metal atom is connected to one ligand molecule and can more fully donate π-electrons to the ligand. Therefore, presumably, the methyl signal that is shifted upfield to the highest extent ($\delta = 0.92$) corresponds to the complex $[Au^{n+}(H_2NCH(Me)CH_2NH_2)](CO_3^{2-})_{0.5n}$ **9d**, while the least shifted signal ($\delta = 1.12$.) corresponds to $[Au^{n+}(H_2NCHMeCH_2NH_2)_4](CO_3^{2-})_{0.5n}$ **9a** (see Fig. 4, *b*). The predominant formation of complex **9a** (65% in the mixture) is apparently a consequence of the kinetic control of this reaction, in which the current concentration of free 1,2-diaminopropane **8** (1 mol L^{-1}) in the solution substantially (~1000-fold) exceeds the gold concentration (~$1 \cdot 10^{-3}$ mol L^{-1}) and the metal atom does not experience a deficiency of the ligand.

The signal of the CH_2 protons in the ^{1}H NMR spectra of both starting 1,2-DAP **8** and the ligands of complexes **9a—d** was recorded as a doublet of doublets. The splitting pattern corresponded to a two-spin ABX system in which non-equivalent CH_A and CH_B protons interact with each other and also with the C<u>H</u> proton of the neighboring

chiral carbon atom (see Fig. 4, *a* and *b*). This signal undergoes a downfield shift (Δδ) relative to that of starting 1,2-diaminopropane **8**, caused by polarization of the CH_2—N bond upon complex formation, which amounts to −0.35 ppm for **9a** and **9b**, −0.05 ppm for **9c**, and −0.20 ppm for **9d**.

For the CH_A and CH_B protons, the spin–spin coupling constants both with each other (^2J) and with the CH protons (^3J) were found to change relative to those of free 1,2-DAP. In the case of compound **9a**, the CH_A coupling constants increase, Δ^2J = 2.0 Hz and Δ^3J = 2.2 Hz, while for the CH_B proton, Δ^2J = 2.0 Hz increases and Δ^3J = −1.2 Hz decreases relative to those of free 1.2-DAP **8**. Simultaneously, the line width between CH_A and CH_B increases by Δν = 8.9 Hz. These changes are due to distortion of the N—C—C bond angle on going from the linear 1,2-diaminopropane **8** molecule to the cyclic molecule of **9a**. Furthermore, they confirm the formation of coordination bonds between the gold atom and both amino groups of 1,2-DAP.

The signal of the (Me)C<u>H</u> proton of the ligand in the ^{1}H NMR spectra of all four complexes **9a—d** is a multiplet at 3.2—3.3 ppm. It is shifted downfield by Δδ = −0.26 relative to that of free 1,2-DAP, as usually observed upon complex formation. Thus, there is no back donation effect of gold π-electrons to the C<u>H</u>$_2$— and C<u>H</u>—protons of the ligand.

In the ^{13}C NMR spectrum of the corrosion product of the gold anode, the methyl carbon atom also gives rise to four signals at 16.8, 18.5, 19.2, and 19.4 ppm, which are shifted upfield relative to the carbon signal of this group in free 1,2-DAP (21.2 ppm) by Δδ = 4.4, 2.7, 2.0, and 1.9 ppm, respectively (Fig. 5, *a*, *b*, see Table 1). This shift confirms the formation of four gold complexes with 1,2-diaminopropane **9a—d** during electrolysis. According to empirical analysis of the integrated intensities of ^{13}C NMR signals of methyl groups, the signal positions along the field (ppm) axis are opposite to those of ^{1}H NMR signals of the protons bound to these carbons. For example, the methyl carbon signal of the predominating complex **9a** (δ = 16.8 ppm) has the greatest upfield shift Δδ = 4.4 (see Fig. 5, *b*), whereas the upfield shift of methyl protons of ligand **9a** observed in the ^{1}H NMR spectrum is minimum among the four complexes **9a—d** and amounts to Δδ = 0.09 (see Fig. 4, *b*). This is probably attributable to the increase in the degree of shielding of the methyl carbon of the ligand with increasing number of the ligand molecules in the complex, with the back donation effect of gold π-electrons to the ligand being retained.

The CH_2 carbon signal of the ligand in the ^{13}C NMR spectrum of the predominating complex **9a** (δ = 46.0) also shows an upfield shift Δδ = 4.1 relative to free 1,2-DAP (δ = 50.1). Meanwhile, the position of the <u>C</u>H carbon signal of the ligand in complex **9a** does not change with respect to that in free 1,2-DAP, being still δ = 49.4.

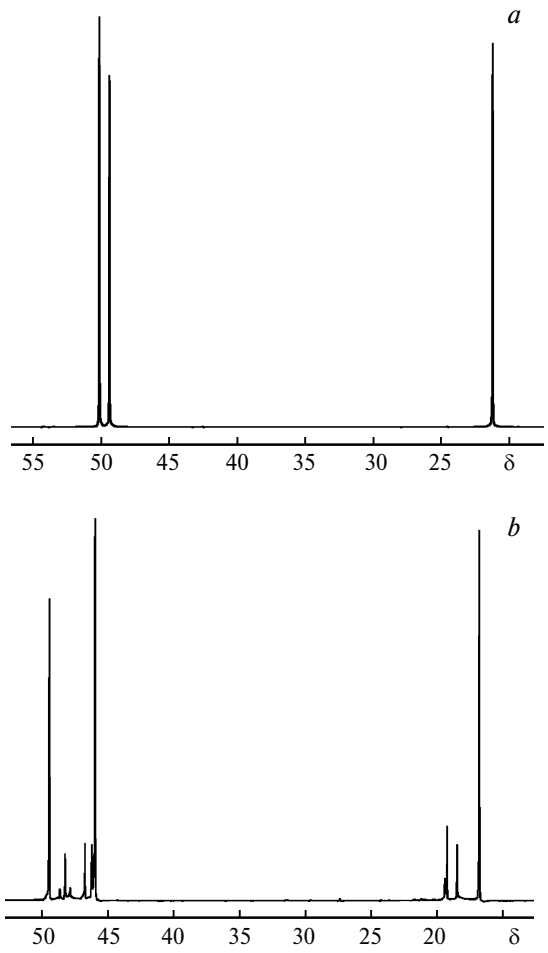

Fig. 5. Fragments of the ^{13}C NMR spectra of 1,2-diaminopropane **8** in D_2O (*a*) and complexes $[Au^{n+}(H_2NCH(Me)CH_2NH_2)_m](CO_3^{2-})_{0.5n}$ (**9a—d**) in D_2O (*b*).

A similar situation is also observed for coordination compounds **9a—d** (see Table 1, Fig. 5).

Despite the fact that, according to NMR spectroscopy, the product of gold electrolysis in a solution of 1,2-diaminopropane **8** is a mixture of four coordination compounds, the IR spectrum of this product contains clear-cut bands, which can be unambiguously interpreted (Fig. 6).

In the NH_2 stretching region, the IR spectrum of the product of electrolysis exhibits a characteristic low-frequency shift of the principal antisymmetrical stretching mode $\nu_{as}(NH_2)$ from 3355 cm^{-1} in free 1,2-DAP to 3310 cm^{-1} in the complex ($\Delta\nu_{as}$ = 45 cm^{-1}). In the region of symmetrical NH_2 stretching vibrations, a characteristic high-frequency shift of the principal $\nu_s(NH_2)$ band from 3282 cm^{-1} in 1,2-DAP to 3310 cm^{-1} in the complex ($\Delta\nu_s$ = 28 cm^{-1}) takes place. These shifts attest to the formation of coordination bonds between the ligand NH_2 groups and the gold atom.[19,20] The involvement of the amino group in the coordination is also evidenced by the high-frequency shift of the $\omega(NH_2)$ bending wagging mode

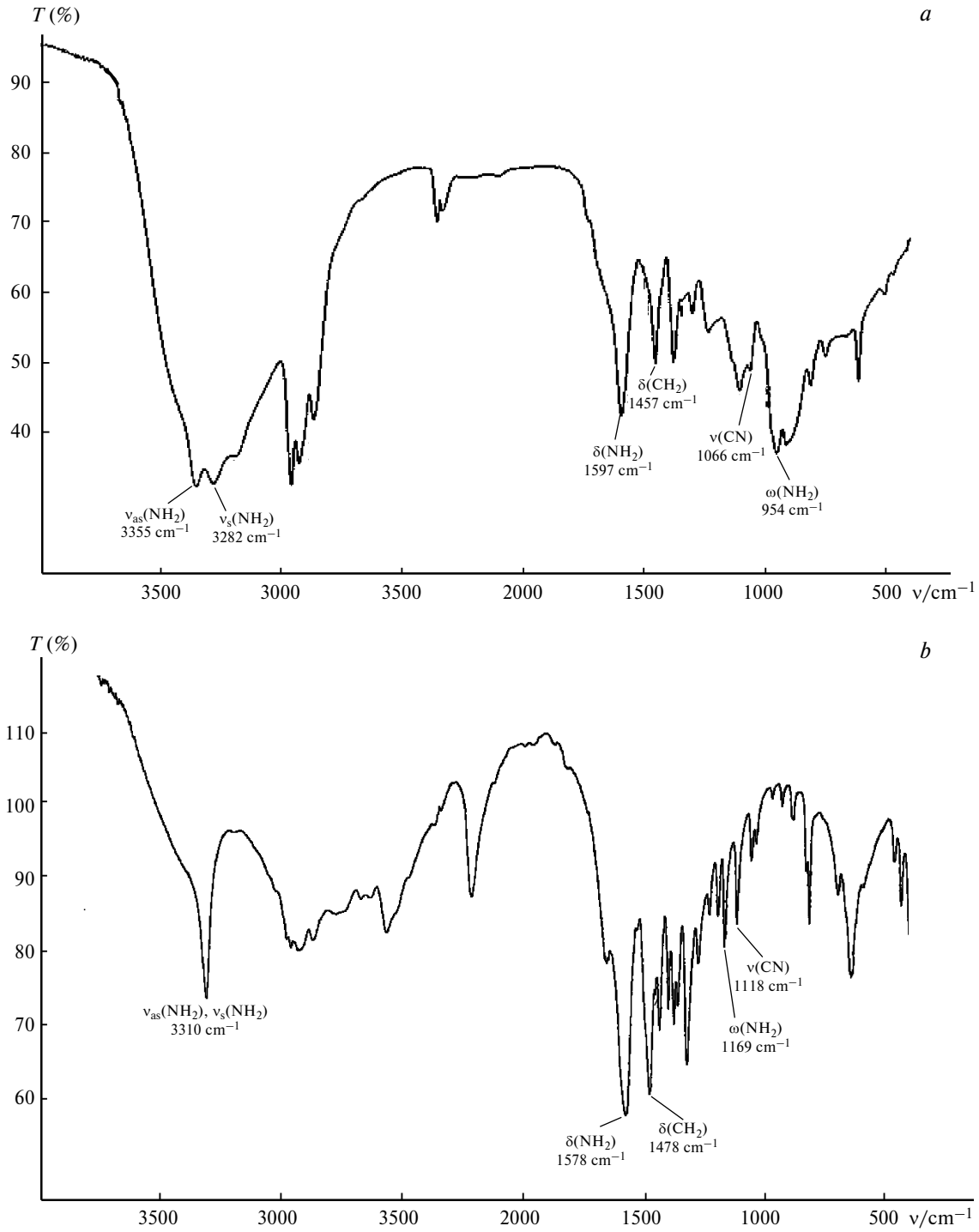

Fig. 6. IR spectra of 1,2-diaminopropane **8** (*a*) and complexes $[Au^{n+}(H_2NCH(Me)CH_2NH_2)_m](CO_3^{2-})_{0.5n}$ (**9a—d**) (*b*).

from 954 cm^{-1} in 1,2-DAP to 1169 cm^{-1} in the product of electrolysis ($\Delta\omega = 215$ cm^{-1}). A similar shift of $\omega(NH_2)$ to a higher frequency from 940 to 1164 cm^{-1} was found in the spectra of complexes of Cu^{2+} ethylenediamine salts[21] and the shift from 915 to 1161 cm^{-1} was observed in the IR spectra of gold complexes with ethylenediamine.[12]

The IR spectra of electrolysis products (a mixture of complexes) also exhibit a characteristic shift of the $\delta(NH_2)$ bending scissoring mode to lower frequency: from 1597 cm^{-1} in free 1,2-DAP to 1578 cm^{-1} in the coordination compound ($\Delta\delta$ = 19 cm^{-1}) and a shift to higher frequency of the ν(C—N) stretching mode from 1066 cm^{-1}

to 1118 cm^{-1}, respectively ($\Delta\nu = 52$ cm^{-1}). Similar shifts of absorption bands were observed, for example, in the IR spectrum of 1,2-bis(2-aminoethyl)diaziridine complex with transition metal salts.[22,23] In the IR spectrum of the electrolysis product, the $\delta(CH_2)$ scissoring bending mode also typically shifts to higher frequency from 1457 cm^{-1} for free 1,2-DAP to 1478 cm^{-1} for **9a—d** ($\Delta\delta = 21$ cm^{-1}).

The ^1H NMR data suggest that the electrolysis product is a mixture of four coordination compounds characterized by different metal-to-ligand ratios: 1 : 4, 65%; 1 : 3, 15%; 1 : 2, 15%; and 1 : 1, 5% (see Fig. 4, *b*). According to calculations using the percentage of each complex in the mixture, the total nitrogen content in all complexes is 20.72%. According to the elemental analysis of a sample representing a mixture of the coordination compounds, the nitrogen content is 21.1%. The agreement between the nitrogen contents together with NMR spectral data confirm the above percentages of the complexes with different metal-to-ligand ratios.

The probable structure of the complex $[Au^{n+}(H_2NCHMeCH_2NH_2)_4](CO_3^{2-})_{0.5n}$ **9a**, in which the gold atom is coordinated to four 1,2-diaminopropane **8** ligands and has a coordination number of 8, is depicted in Fig. 7. This high coordination number of gold does not contradict the literature data. For example, it was shown[24] that CN of 12 is possible.

The intense formation of colloidal metallic gold particles observed during electrolysis of a 1,2-DAP solution is probably due to low stability of complexes **9a—d** caused by the lack of symmetry of the ligand molecule, which leads to different N---Au bond energies for different nitrogen atoms of the complex.

Thus, our study (carried out by gravimetric method) demonstrated that in weakly basic aqueous solutions of 1,2-diaminopropane **8**, a gold anode underwent corrosion, like in similar processes with other aliphatic diamines. Under galvanostatic conditions, the corrosion products are reduced on the steel cathode to give an electrolytic gold deposit.

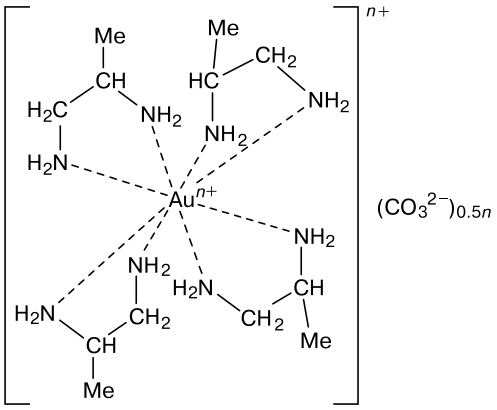

Fig. 7. Probable structure of the complex $[Au^{n+}(H_2NCH(Me)CH_2NH_2)_4](CO_3^{2-})_{0.5n}$.

Transmission electron microscopy examination revealed the presence of colloidal gold nanoparticles in the electrolyte solution, similarly to the chemical synthesis of these particles.[25] In our case, the formation of colloidal gold is apparently associated with low stability of gold complexes with 1,2-DAP, caused by the unsymmetrical structure of the ligand. Thus, gold formed upon the cathode reduction of the complex can remain in the electrolyte solution. In addition, a mixture of four gold complexes with 1,2-diaminopropane **8**, differing in the number of ligand molecules bound to the Au atom, was isolated by methanol extraction of the electrolyte solution. The complex formed predominantly has the composition $[Au^{n+}(H_2NCH(Me)CH_2NH_2)_4](CO_3^{2-})_{0.5n}$. The results of our study of the anodic corrosion of gold in solutions of aliphatic diaminoalkanes provide the conclusion that aliphatic diamines are able to form gold complexes, which are then transferred and give a gold deposit on the cathode. The appearance of colloidal gold in this process opens up the possibility to choose the most appropriate ligands for targeted synthesis of solid (or colloidal) gold.

The authors are grateful to the Department of Structural Studies of the N. D. Zelinsky Institute of Organic Chemistry, Russian Academy of Sciences. for electron microscopic examination of the samples.

Reference

1. G. Zelinsky, *Electrochim. Acta,* 2015, **154**, 315.
2. G. Zelinsky, O. N. Novgorodtseva, *Electrochim. Acta*, 2013, **109**, 482.
3. S. Zhang, M. J. Nicol, *J. Appl. Electrochem.,* 2003, **33**, 767.
4. M. Tian, B. E. Conway, *J. Appl. Electrochem.*, 2004, **34**, 533.
5. S. Zhang, M. J. Nicol, *J. Appl. Electrochem.,* 2005, **35**, 339.
6. X. Yang, M. S. Moats, J. D. Miller, *Electrochim. Acta,* 2010, **55**, 3643.
7. S. R. Smith, E. Guerra, S. Siemann, J. L. Shepherd, *Electrochim. Acta*, 2011, **56,** 8291.
8. A. P. Simakova, M. D. Vedenyapina, V. V. Kuznetsov, N. N. Makhova, A. A. Vedenyapin, *Russ. J. Phys. Chem. A*, 2014, **88**, 331.
9. M. D. Vedenyapina, V. V. Kuznetsov, N. N. Makhova, A. A. Vedenyapin, *Russ. J. Phys. Chem. A*, 2016, **90**, 1903.
10. M. D. Vedenyapina, G. Ts. Ubushieva, V. V. Kuznetsov, N. N. Makhova, A. A. Vedenyapin, *Russ. J. Phys. Chem. A*, 2016, **90**, 2312.
11. M. D. Vedenyapina, V. V. Kuznetsov, D. I. Rodikova, N. N. Makhova, A. A. Vedenyapin, *Mendeleev Commun*., 2018, **28**, 181.
12. M. D. Vedenyapina, V. V. Kuznetsov, N. N. Makhova, D. I. Rodikova, *Russ. J. Phys. Chem. A*, 2019, **93**, 466.
13. M. D. Vedenyapina, V. V. Kuznetsov, N. N. Makhova, D. I. Rodikova, *Russ. Chem. Bull.* (*Int. Ed.*), 2019, **68**, 1997.
14. V. V. Kachala, L. L.Khemchyan, A. S.Kashin, N. V.Orlov, A. A.Grachev, S. S.Zalesskiy, V. P.Ananikov, *Russ. Chem. Rev.*, 2013, **82**, 648.
15. Pat. WO/2011/158176 dated 22.12.2011.

16. D. M. Khramov, V. M. Lynch, C. W. Bielawski, *Organomet. Chem.*, 2007, **26**, 6042.
17. J. A. Flores, H. V. Rasika Dias, *Inorg. Chem.*, 2008, **47**, 4448.
18. D. Marchione, L. Belpassi, G. Bistoni, A. Macchioni, F. Tarantelli, D. Zuccaccia, *Organomet. Chem.,* 2014, **33**, 4200.
19. A. G. Bulakh, A. A. Zolotarev, V. G. Krivovichev, *Obshchaya mineralogiya* [*General Mineralogy*], Akademiya, Moscow, 2008, 416 pp. (in Russian).
20. I. B. Bersuker, *Elektronnoe stroenie i svoistva koordinatsionnykh soedinenii* [*Electronic Structure and Properties of Coordination Compounds*], Khimiya, Leningrad, 1986, 288 pp. (in Russian).
21. N. K. Hall, *J. Am. Chem. Soc.*, 1957, **20**, 5441.
22. K. Dwara Kanath, D. N. Sathyanarayana, *Bull. Soc. Chim. Belg.*, 1978, **87**, 677.
23. V. P. Sinditskii, M. D. Dutov, A. E. Fogel´zang, V. V. Kuznetsov *Zh. Neorg. Khim.*, 1991, **36**, 944 [*Sov. J. Inorg. Chem.*, 1991, **36**].
24. A. V. Shevtsov, V. Yu. Petukhova, S. A. Kutepov, V. V. Kuznetsov, N. N. Makhova, N. E. Kuz´mina, G. G. Aleksandrov, *Russ. Chem. Bull.*, 2000, **49**, 1882.
25. A. A. Revina, K. F. Chernyshova, N. Yu. Tabachkova, Yu. N. Parkhomenko, *Russ. Chem. Bull.*, 2019, **68**, 1164.

Received December 26, 2019;
in revised form March 20, 2020;
accepted July 28, 2020